JOURNAL OF SOLID STATE CHEMISTRY 120, 244–253 (1995)

Electronic Spectrum and Antiferromagnetic *A–B* Interactions between Tetrahedral $3d^5$ and $3d^5$ or $3d^3$ Octahedral Cations in Oxidic Lithium Spinels

F. Hochu,* M. Lenglet,*,[1] and C. K. Jørgensen†

*Laboratoire d'Analyse de Spectroscopie et de Treatment de Surface des Matériaux, Université de Rouen, I.U.T., 76821 Mont Saint Aignan, France; and †Université de Genève, Département de Chimie Minérale Analytique et Appliquée, 30 Quai Ernest Ansermet, CH-1211 Geneva 4, Switzerland

Received February 17, 1995; in revised form July 3, 1995; accepted July 6, 1995

The compounds chosen to illustrate the interpretation of ligand field spectra of inorganic solids with *A–B* antiferromagnetic coupling between Fe^{3+} tetrahedral and Fe^{3+} or Cr^{3+} octahedral cations belong to the $Li_{0.5}Fe_xGa_{2.5-x}O_4$ and $Li_{0.5}(FeCr)_xGa_{2.5-2x}O_4$ systems. New features, such as the interpretation of the iron(III) electronic spectrum in ferrimagnetic spinels, the influence of the nature of the superexchange interactions of the pair excitation processes, and the growth of an electronic transition assigned to $Cr^{3+} + Fe^{3+} \rightarrow Cr^{4+} + Fe^{2+}$ intervalence charge transfer at 1.8 eV are reported in this study. © 1995 Academic Press, Inc.

I. INTRODUCTION

The optical spectra of transition-group metal ions have been the subject of intense investigations attempted in order to obtain a fundamental understanding of the varied colors and luminescent properties exhibited by these ions in different crystalline environments. However, with very few exceptions, the studies have been confined to spectra that arise as a result of "internal" transitions. Some much more intense absorptions are due to electron transfer: ligand–metal charge transfer (LMCT), intervalence charge transfer (IVCT), or metal–metal charge transfer (MMCT). The purpose of this paper is to present the influence on optical spectra of superexchange interactions between Cr^{3+} and Fe^{3+} in the spinel structure.

The compounds chosen to illustrate the interpretation of ligand field spectra of inorganic solids with *A–B* antiferromagnetic coupling between Fe^{3+} tetrahedral and Fe^{3+} or Cr^{3+} octahedral cations belong to the $Li_{0.5}Fe_xGa_{2.5-x}O_4$ and $Li_{0.5}(FeCr)_xGa_{2.5-2x}O_4$ systems.

New features, such as the interpretation of the iron(III) electronic spectrum in ferrimagnetic spinels, the influence of the nature of the superexchange interactions on the pair excitation processes, and the growth of an electron transition assigned to $Cr^{3+} + Fe^{3+} \rightarrow Cr^{4+} + Fe^{2+}$ intervalence charge transfer at 1.8 eV are reported in this study.

II. EXPERIMENTAL

Different series of lithium spinels were prepared by means of a simple ceramical method by mixing suitable proportions of Li_2CO_3, Cr_2O_3, and appropriate M_2O_3 oxide (M = Ga or/and Fe) and twofold sintering at 800 and 1100°C in an air atmosphere. The samples slowly cooled at 10°C · hr^{-1} were checked by X-ray diffraction. Some iron(III) spinels were analyzed by Mössbauer spectroscopy. Diffuse reflectance spectra in the UV–visible and near-infrared were obtained using a Perkin-Elmer Lambda9 spectrophotometer equipped with an integrating sphere accessory and a 7300 computer (the integrating sphere was coated with $BaSO_4$ and the spectra were referenced against $BaSO_4$). For an easier comparison in the visible region, the spectra of the lithium ferrigallates (Fig. 1a and 1b) were converted to the Kubelka–Munk remission function defined by

$$F(R) = \frac{(1-R)^2}{2R} = \frac{k}{s},$$

where R is the reflectance and k is the absorption coefficient. Assuming that the scattering coefficient s has only a small variation with the wavelength over the range of interest, the shapes of the remission function and absorption spectrum are identical. Difference spectra and electronic spectra of $Li_{0.5}Cr_xGa_{2.5-x}O_4$ and $Li_{0.5}(FeCr)_xGa_{2.5-2x}O_4$ solid solutions are presented in absorbance.

[1] To whom correspondence should be addressed.

0022-4596/95 $12.00

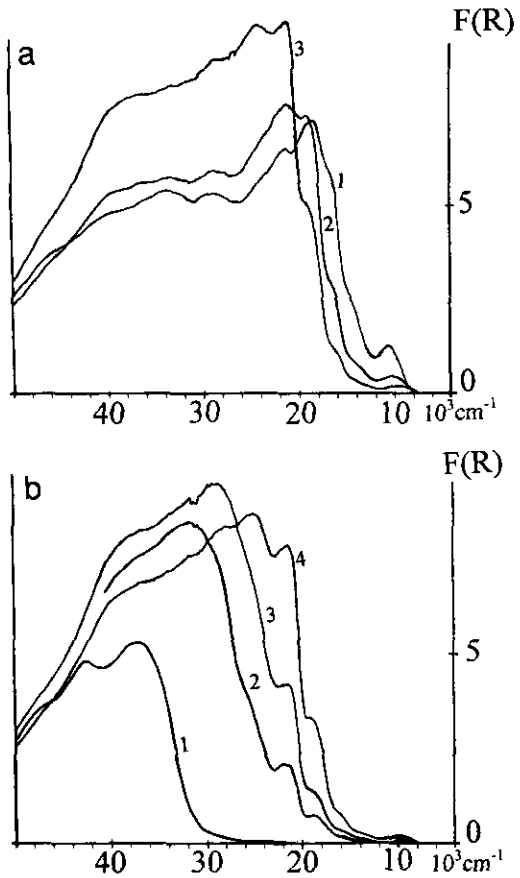

FIG. 1. NIR–Visible and near ultraviolet absorption spectra of ferrimagnetic (a) and paramagnetic (b) compounds in the $Li_{0.5}Fe_xGa_{2.5-x}O_4$ system. (a) 1, x = 2.5; 2, x = 2; and 3, x = 1.5. (b) 1, x = 0.05; 2, x = 0.5; 3, x = 1; and 4, x = 1.25. (The energies and assignments of the observed bands are presented in Table 2).

III. EXPERIMENTAL RESULTS AND INTERPRETATIONS

III.1. Influence of Superexchange Interactions on the Optical Spectra of Fe^{3+} and Cr^{3+} Ions in Spinels

$Li_{0.5}Ga_{2.5-x}M_xO_4$ Systems

$Li_{0.5}Ga_{2.5-x}Fe_xO_4$. The lithium ferrigallates are ordered inverse spinels with long-range order 1:3 in the octahedral sublattice. The cation distribution is

$$Fe^{3+}_{x_A}Ga^{3+}_{1-x_A}[Li^{+}_{0.5}Fe^{3+}_{x_B}Ga^{3+}_{1.5-x_B}]O_4 \; x_A + x_B = x.$$

For $x > 1.5$, the Ga^{3+} ions show a marked preference for A sites. In these mixed oxides the ordered arrangement of Li^+ and M^{3+} ions on the B sublattice is conserved while the order is absent among M^{3+} ions in each sublattice (1). The main data related to the cation distribution are in good agreement:

x									
0.25	0.5	1	1.25	1.4	1.5	2	2.5		Ref.
				x_B/x_A		2.08		XRD, m.m.	(1)
		1.63	2.05		2.26	1.90	1.5	XRD, m.m.	(2)
				2.41		2.03		MS	(3)
			1.93					MS	(4)
0.79	1.5							MS	This study

XRD, X-ray diffraction, m.m., magnetization measurements; MS, Mössbauer spectroscopy.

The magnetic structure of the ferrimagnetic compounds ($x \geq 1.25$) is not actually solved. Using Mössbauer spectroscopy, Bashkirov *et al.* (5) investigated the effect of gallium substitution on the nature of the superexchange interactions and concluded that as the Ga^{3+} content is increased, the intrasublattice interactions become stronger and the intersublattice interactions weaken because of the reduction in lattice parameters; this facilitates a canted spin alignment at the octahedral sites. They also suggested that the Ga^{3+} ions are involved in the chain of intersublattice interactions due to the transmittance of finite spin density from the Fe^{3+} ions into the empty 4*s* orbitals of Ga^{3+} ions. This conclusion was mainly derived from the results of Doroshev *et al.* (6) who showed the existence of significant transferred hyperfine fields at the Ga^{3+} sites from the ^{71}Ga and ^{69}Ga NMR studies of this system, $x \geq 1.84$. Belov *et al.* (4) deduced from the magnetization study of $Li_{0.5}Fe_{1.23}Ga_{1.27}O_4$ the possibility of a canted spin alignment even for the tetrahedral sites. Other authors have shown that the spin canting exists only for the octahedral sites using Mössbauer spectroscopy with and without an external magnetic field (3) or neutron diffraction (7).

The luminescence of Fe^{3+} in oxide lattices has received much attention in the literature. The spinels $Li_{0.5}M_{2.5}O_4$ (M = Al and Ga), when lightly doped with Fe^{3+} ions, exhibit an emission assigned to the $^4T_1(^4G) \rightarrow {}^6A_1(^6S)$ electronic transition of this center for an A-site occupancy (8–11).

Table 1 gives the experimental values for the ligand field transitions of the $Fe^{3+}:Li_{0.5}Al_{2.5}O_4$ and $Fe^{3+}:Li_{0.5}Ga_{2.5}O_4$ systems, the crystal field parameter $10Dq$ and the Racah parameters B and C deduced from the Tanabe–Sugano crystal field theory.

The assignments proposed in references (9) and (10) are obviously wrong as well as the conclusions established by Abritta (12) from photoacoustic measurements of $Li_{0.5}Ga_{2.5-x}Fe_xO_4$ samples containing Fe^{3+} impurity concentrations in the range 3.0 to 5.0 at.%. These authors consider that up to the concentrations used, the iron(III) mostly occupies the octahedral sites and the photoacoustic bands are associated to these centers, whereas the luminescent features are associated to some residual Fe^{3+} ions in tetrahedral sites (the attribution of the photoacoustic spectrum

TABLE 1
Optical Properties of Fe^{3+a} in $Li_{0.5}M_{2.5}O_4$ Spinels

	Energy (in 10^3 cm^{-1}) of the observed transitions					Optical parameters (in 10^3 cm^{-1})			
	$^6A_1 \rightarrow {}^4T_1$	$^4T_2$	$^4E_1{}^4A_1$	$^4T_2$	^4E	$10Dq$	B	C	Ref.
$Fe^{3+}:Li_{0.5}Al_{2.5}O_4$	15.25	18.7	21.3	22.55	25.72	8	0.645	2.96	(8)
	19.08	22.47	25.72	28.33	30.19	9.5	0.64	3.87	(9, 10)
	15.75	19.08	21.11	22.22	25.51	7.7	0.605	3.05	(11)
$Fe^{3+}:Li_{0.5}Ga_{2.5}O_4$	18.35	21.51	24.63	27.04	28.80	9.1	0.595	3.74	(10)
	14.55	17.8	21.05	22.86	25.48	9.1*	0.585	3.04	(12)

[a] Fe^{3+} octahedral.

to Fe^{3+} octahedral is accurate but the band assignments and, consequently, the calculated optical parameters must be revised).

The optical properties of lithium and magnesium ferrites are interpreted as follows by Zhang *et al.* (13): up to 4 eV, the optical absorption is due to Fe $3d^n \rightarrow 3d^{n-1}$ $4s$ orbital promotion processes including final state effects of the atom like $3d^{n-1}$ configurations and above 5 eV it is due to oxygen $2p$ band to iron $4s$ band charge transfer transitions.

The substitution for the tetrahedral and octahedral Fe^{3+} ions by nonmagnetic Ga^{3+} ions provides a possibility for experimentally distinguishing transitions from various sites. The observed band energies and their assignments are summarized in Table 2.

From the $^6A_1 \rightarrow {}^4T_1(^4G)$ or $^4T_2(^4G)$, $^6A_1 \rightarrow {}^4E_1{}^4A_1(^4G)$ and $^6A_1 \rightarrow {}^4E(^4D)$ transition energies and the Tanabe–Sugano equations, the ligand field parameters can be calculated and the values obtained can be used in order to determine the energies of the remaining transitions. The predicted energies of the pair excitation bands for octahedral Fe^{3+} ions are obtained assuming that they are equal to the sum of the two ligand field transition energies (as observed experimentally, this may sometimes be only a rough approximation).

Since the $^6A_1 \rightarrow ({}^4E_1{}^4A_1)$ and $^6A_1 \rightarrow {}^4E$ transitions are not split, the B and C values are the same for the two tetrahedral and octahedral environments of iron(III).

The experimental values of $10Dq$, B, and C for $x \leq 0.5$ are in excellent agreement with those found in the literature for spinels compounds with Fe^{3+} in tetrahedral coordination (8, 11, 16) and octahedral coordination (16) in Table 3.

In the near infrared region, the spectra are characterized by the presence of the $^6A_1 \rightarrow {}^4T_1(^4G)$ Fe^{3+} octahedral transition. The position of this transition depends strongly

TABLE 2
Energies and Assignments of Bands Observed in the $Li_{0.5}Fe_xGa_{2.5-x}O_4$ Spectra

Transitions	Observed and (calculated) electronic transitions energies (in 10^3 cm^{-1})							
x =	0.05	0.25	0.5	1	1.25	1.5	2	2.5
$^6A_1 \rightarrow {}^4T_1$Oh	9.3	9.4 (9.4)	9.35	9.4	9.7	9.7	10.2	10.6
$^6A_1 \rightarrow {}^4T_2$Oh	~13.4	~13.4 (13.8)	13.5	13.6	14	14	14.5	14.5
$^6A_1 \rightarrow {}^4T_1$Td	~15.8	~15.8	16	16	16.2	16.2	16.4	16.1–16.3
$2(^6A_1) \rightarrow 2(^4T_1)$ $^6A_1 \rightarrow {}^4T_2$(Td)	~18.9	19 (19)	19	19.2	19.2	19.2	19*	18.4–19*
$^6A_1 \rightarrow {}^4E_1{}^4A_1$	21.2	21.2 (21.2)	21.2	21.2	21.2	21.2	21.2	21.2
$^6A_1 \rightarrow {}^4T_2(D)$	22	22 (23.2)	22	22				
$^6A_1 \rightarrow {}^4E(D)$	~26	25.8 (25.8)	25.5		25*	24.2*		
$2(^6A_1) \rightarrow 2(^4T_2)$ $2(^6A_1) \rightarrow (^4E_1{}^4A_1) + {}^4T_1$		29		29	28	28	28.5	29
$^6A_1 \rightarrow {}^4T_1(P)$		(33)	32				34.5	34
LMCT	37.2	~36	~36	~37	37	37	34.5	34

Note. 19 main band, 19* and 25* composite of two transitions (see text); Td, tetrahedral; Oh, octahedral.

TABLE 3
Optical Parameters (in 10^3 cm^{-1}) of Tetrahedral and Octahedral Iron(III) in Spinels

Compound	Fe^{3+} Td			Fe^{3+} Oh			Ref.
	$10Dq$	B	C	$10Dq$	B	C	
$Li_{0.5}Fe_{0.25}Ga_{2.25}O_4$	8.3	0.66	2.92	14	0.66	2.92	This study
$Fe^{3+}:Li_{0.5}Al_{2.5}O_4$	8	0.64_5	2.96				(8)
	7.7	0.60_5	3.05				(11)
$ZnFe_{0.05}Ga_{1.95}O_4$				15.75	0.6	3.12	(16)
$MgFe_{0.1}Ga_{1.9}O_4$	8.9	0.67	2.9				(16)

on the crystal field strength. With increasing crystal field the transition shifts to lower energy. Spectral bands at higher energies than 16,000 cm^{-1} are much more intense than the transitions related to the $(t_{2g}^{\alpha})^3(e_g^{\alpha})^1(t_{2g}^{\beta})^1$ configuration and give a steep absorption edge. In ferrimagnetic compounds (Fig. 1a), the band located at 21,200 cm^{-1} is very strong and well-defined. The energy of this transition corresponds to that of the $^6A_1 \rightarrow {}^4E_1{}^4A_1$ ligand field transition in spinels (in tetrahedral or octahedral coordination (8, 11, 16)). In lithium ferrite and $Li_{0.5}Fe_2Ga_{0.5}O_4$, the band at 19,000 cm^{-1} may be attributed to the $^6A_1 \rightarrow {}^4T_2$ transition of the tetrahedral iron(III) and to the $^6A_1 + {}^6A_1 \rightarrow {}^4T_1({}^4G) + {}^4T_1({}^4G)$ transition characteristic of the pair excitation process. For $x = 1.25$ and 1.5, the spin flip transition (^4E) is hidden by the $^6A_1 + {}^6A_1 \rightarrow {}^4T_1({}^4G) + {}^4T_2({}^4G)$ transition. The band at 28,000–29,000 cm^{-1} is either the $^6A_1 + {}^6A_1 \rightarrow {}^4T_2({}^4G) + {}^4T_2({}^4G)$ transition in ferrimagnetic compounds or the $^6A_1 + {}^6A_1 \rightarrow {}^4E_1{}^4A_1({}^4G) + {}^4T_1({}^4G)$ transition in paramagnetic samples ($x \leq 1$). With decreasing x values the absorption edge is shifted to higher energies (i.e., from 1.5 eV in $Li_{0.5}Fe_{2.5}O_4$ to 2.5 eV in paramagnetic compounds). As in αFe_2O_3, the $^6A_1 \rightarrow {}^4E_1{}^4A_1({}^4G)$ and $^6A_1 + {}^6A_1 \rightarrow {}^4T_1 + {}^4T_1$ transitions are strongly intensified in lithium ferrite and high Curie temperature compounds. The spectra of materials having lower Curie temperature ($Li_{0.5}Fe_{1.5}Ga_1O_4$: θ_c = 175°C, $Li_{0.5}Fe_{1.25}Ga_{1.25}O_4$: θ_c = 70°C) are characterized by a large enhancement of the $^6A_1 \rightarrow {}^4E_1{}^4A_1$ and $^6A_1 + {}^6A_1 \rightarrow {}^4T_1 + {}^4T_2$ (near 24,000 cm^{-1}) transitions. The paramagnetic compounds (at room temperature) present a spectrum similar to that of $ZnFe_2O_4$ (for octahedral iron(III)): a strong intensification of the $^6A_1 + {}^6A_1 \rightarrow {}^4E_1{}^4A_1({}^4G) + {}^4T_1({}^4G)$ transition near 29,000 cm^{-1} is observed.

In order to get a better understanding of this evolution of the electronic spectrum, we have studied the variation of different ratios (Table 4) like $I_{16000}/[Fe^{3+}_{tetra}]$, where I_{16000} the intensity at 16,000 cm^{-1}, is measured on the reflectance spectrum converted to the Kubelka–Munk function, and $[Fe^{3+}_{tetra}]$ is the iron(III) content on tetrahedral sites.

From the above-mentioned data, the following conclusions may be drawn:

— The ligand field transitions unaffected by a double exciton process are strongly enhanced by the A–B interactions.

— The band at 19,000 cm^{-1} is unambiguously a composite of the $^6A_1 \rightarrow {}^4T_2({}^4G)$ ligand field transition of tetrahedral Fe^{3+} and $^6A_2 + {}^6A_1 \rightarrow {}^4T_1 + {}^4T_1({}^4G)$ pair transition.

— The gallium substitution in lithium ferrite influences the nature of interactions: as the gallium content is increased, the intersublattice interactions weaken and the intrasublattice interactions become stronger facilitating a canted spin alignment on the octahedral sites. This phenomenon induces a strong intensification of pair transitions: $^6A_1 + {}^6A_1 \rightarrow {}^4T_1 + {}^4T_2({}^4G)$ and $^6A_1 + {}^6A_1 \rightarrow ({}^4E_1{}^4A_1) + {}^4T_1({}^4G)$.

— In paramagnetic compounds, the absorption coefficient k for the Fe^{3+} ion in tetrahedral coordination is ten times higher than that of octahedral Fe^{3+}.

	$Li_{0.5}Fe_{0.5}Ga_2O_4$	$MgFe_{0.4}Ga_{1.6}O_4$
I_{14000}/Fe^{3+}_{octa}	0.18	0.22
$I_{19000}/Fe^{3+}_{tetra}$	3	2.6
k_{tetra}/k_{octa}	~15	~12

In conclusion, new features such as the interpretation of the iron(III) electronic spectrum in spinels, the influence of the nature of the superexchange interactions on the pair excitation processes, and the values of the absorption coefficient for the two Fe^{3+} species are reported for the first time in this study. Band assignments and crystal-field parameters are in agreement with the results of the self-consistent field-Xα-scattered wave (SCF-Xα-SW) molecular calculations of (FeO_6^{9-}) and (FeO_4^{5-}) coordination polyhedra (17). The proposed interpretation of the electronic spectrum of iron(III) in ferrimagnetic spinels ($MgFe_2O_4$, $Li_{0.5}Fe_{2.5}O_4$) rules out the MMCT charge transfer model ($2Fe^{3+} \rightarrow Fe^{2+} + Fe^{4+}$) considered by numerous authors in order to explain the photoelectrochemical properties of these materials (18–20).

$Li_{0.5}Cr_xGa_{2.5-x}O_4$. In the $Li_{0.5}Ga_{2.5-x}Cr_xO_4$ ($x \leq 2$) extensively studied (21–23), two order–disorder transitions $P4_332 \rightarrow Fd3m$ and $F\bar{4}3m \rightarrow Fd3m$ occur, respectively, for $x = 1.25$ and $x = 1.75$ (these transitions are connected with the migration of lithium from octahedral to tetrahedral sites). The optical spectrum of Cr^{3+} in these spinels have been reinvestigated in order to complete the known data about the crystal field in lithium spinels (Fig. 2 and Table 5).

In $Cr^{3+}:Li_{0.5}Al_{2.5}O_4$ (24) and low chromium content spinels of the $Li_{0.5}Cr_xGa_{2.5-x}O_4$ system ($x \leq 0.5$) (23, 25) the crystal field acting on the Cr^{3+} octahedral has a lower symmetry (C_2) than in normal spinel. For $x \geq 0.5$, a very

TABLE 4
Variation of the Intensity of Iron(III) Ligand-Field and Pair Transition Determined on Remission Spectra of $Li_{0.5}Fe_xGa_{2.5-x}O_4$ Solid Solutions near the Magnetic Transition

Ratio	x = 2.5	2.25	2	1.5	1.25	1	0.5
I_{14000}/Fe^{3+}_{octa}	0.87	0.71	0.5	0.4	0.25	0.16	0.18
$I_{16000}/Fe^{3+}_{tetra}$	6	—	4.3	2.6	2.2	1	—
$I_{19000}/Fe^{3+}_{tetra}$	7.5	12	11	9	9	3.8	3
I_{24000}/Fe^{3+}_{octa}	—	—	—	10	9.5	6	~3.5
I_{29000}/Fe^{3+}_{octa}	~3.5	—	4.5	8	~9	8.5	—
θ_c(°C)	620	510	400	280	175	70	—
Canting angle α_{yk}(deg)	0		30	30		~25 (from Ref. 3)	

slight percentage of Cr^{3+} ions is observed in tetrahedral coordination (about 1%) (21).

The spectra can be interpreted as follows.

— $x \leq 0.25$: the spectrum is composed of two broad bands split into two or three sub-bands (o_1 and o_2 are spin-allowed) and weak spin-forbidden bands (o_a and o_b).The bands at 28500 and 30000 cm^{-1} are connected with Cr^{3+}–Cr^{3+} pairs and the intense shoulder near 41000 cm^{-1} is the first LMCT band (Fig. 2, curve 1).

— $0.25 < x < 1.25$: the Cr^{3+} octahedral is unchanged and at lower energy the two spin-allowed bands of Cr^{3+} ions in tetrahedral coordination appear (Fig. 2, curves 2, 3, and 4).

— $x \geq 1.5$: the spectrum is characterized by a strong enhancement of the absorption at 29,500 cm^{-1} attributed to the pair transitions $2(^4A_{2g}) \rightarrow 2(^2E_g)$ and $2(^2T_{1g})$. The third spin-allowed transition of Cr^{3+} octahedral is hidden by the ligand metal charge transfer band (Fig. 2, curve 5).

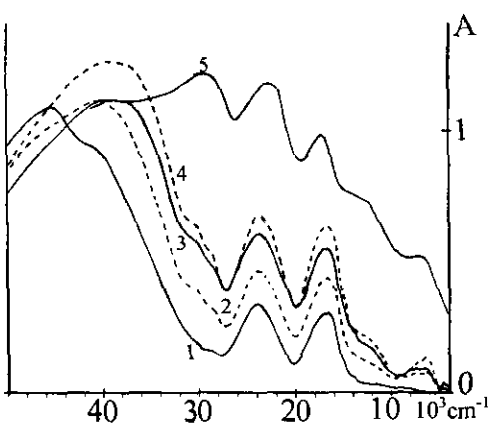

FIG. 2. Electronic spectrum of Cr^{3+} in the $Li_{0.5}Cr_xGa_{2.5-x}O_4$ system. 1, $x = 0.25$; 2, $x = 0.5$; 3, $x = 0.75$; 4, $x = 1$; and 5, $x = 2$. (The energies and assignments of the observed bands are presented in Table 5).

The corresponding values of $10Dq$, B, and C (in 10^3 cm^{-1}) are listed hereafter:

	Cr^{3+}		Cr^{3+} octahedral		
x	$10Dq$	B	$10Dq$	B_{35}	C
0.25			16.75	0.74	3
1.25	~7	0.5	16.8	0.65	3.2
2	~7	0.5	17.3	0.57	

The spinels $Li_{0.5}Cr_1Ga_{1.5}O_4$ and $Li_{0.5}Cr_{1.625}Ga_{0.875}O_4$ in which only B–B interactions are present have been studied magnetically (26). As $ZnCr_2O_4$, they are characterized by low Néel temperatures ($x = 1$: $\theta_N = 4$ K; $x = 1.625$: $\theta_N = 11$ K). The Racah parameter B_{35} determined from the o_2 transition has to do with an excited σ antibonding e_g electron ($t_{2g}^2 e_g^1$) and, as expected, decreases with increasing Cr^{3+} concentration. Similar effects on B_{35} or B have been observed in different systems: $Cr_xAl_{2-x}O_3$ (27), $Ni_xMg_{1-x}O$, and $Co_xMg_{1-x}O$ (28). The study of the optical properties of the Cr^{3+} ion in the $Li_{0.5}Cr_xGa_{2.5-x}O_4$ system shows that the antiferromagnetic coupling between two adjacent cations induces a strong intensification of the pair transitions in chromium rich compounds and the splitting of the $^4A_{2g} \rightarrow {}^2E_g$ transition into a group of lines between 13,950 and 14,200 cm^{-1}.

III.2. Influence of the Superexchange Interactions between Fe^{3+} Tetrahedral and Cr^{3+} Octahedral: The Cr^{3+}–Fe^{3+} Intervalence Charge Transfer in Ferrimagnetic Compounds

$Li_{0.5}(CrFe)_xGa_{2.5-2x}O_4$ System

In a previous paper, we have shown that the 135° Cr–O–Fe antiferromagnetic interactions in the corundum structure and the 125° Fe^{3+}_{tetra}–O–Cr^{3+}_{octa} interactions in the spinel structure induce the growth of a large electronic transition at 1.70 eV assigned to the Cr^{3+}–Fe^{3+} intervalence charge transfer (29).

TABLE 5
Optical Properties of Cr^{3+} in the $Li_{0.5}Cr_xGa_{2.5-x}O_4$ System: Energy and Assignment of the Observed Transitions (10^3 cm^{-1})

	Tetrahedral Cr^{3+}		Octahedral Cr^{3+}								
									$^4T_{1g}(P)$ o_3		
x	$^4T_1 \rightarrow {}^4T_2$	$^4T_1(P)$	$^4A_{2g} \rightarrow {}^2E_g$ o_a	$^2T_{1g}$ o_b	$^4T_{2g}$ o_1	$^2T_{2g}$ o_c	$^4T_{1g}$ o_2	Pairs transitions	Obs.	Calc.	LMCT
0.25			13.95–14.2	~15	16.75	(21.4)	24	28.8–30		37.3	41
1.25	6.5	~13		15	16.8		23.4	29–30.5	36	36.8	40.5
2	6.5	~13			17.3		23.2	~29.5		37.2	

The $Li_{0.5}(CrFe)_xGa_{2.5-2x}O_4$ system is very suitable for the thorough study of this phenomenon. In paramagnetic compounds ($x \leq 0.5$), the iron(III) is equally located on A and B sites and in ferrimagnetic compounds ($x > 0.5$), the iron(III) migrates on the tetrahedral sites because of the increasing chromium content. The cationic distribution deduced from XRD and Mössbauer studies are presented hereafter:

x	Tetrahedral sites	Octahedral sites	Ref.
0.25	$Fe_{0.12}Ga_{0.88}$	$Li_{0.50}Cr_{0.25}Fe_{0.13}Ga_{1.12}O_4$	This study
0.5	$Fe_{0.25}Ga_{0.75}$	$Li_{0.50}Cr_{0.50}Fe_{0.25}Ga_{0.75}O_4$	This study
0.75	$Fe_{0.43}Ga_{0.57}$	$Li_{0.50}Cr_{0.75}Fe_{0.32}Ga_{0.43}O_4$	This study
1	$Fe_{0.70}Ga_{0.30}$	$Li_{0.50}Cr_1Fe_{0.30}Ga_{0.20}O_4$	This study
1.25	$Li_{0.09}Fe_{0.91}$	$Li_{0.41}Cr_{1.25}Fe_{0.34}O_4$	(30)

(The iron distribution is obtained from the deconvolution of the Mössbauer spectrum recorded in the paramagnetic range: at room temperature, for $x = 0.25$ and 0.50 and at 473 K, for $x = 0.75$ and 1.)

IR Study. Infrared vibrational spectroscopy has been used to determine structural units and local symmetries in crystalline and noncrystalline solids. Especially ordering phenomena in spinels have been studied successfully with vibrational spectroscopy (31–34). It was pointed out by White and De Angelis (32) that the vibrational spectrum of the spinel structure can be treated by a factor group analysis, which predicts four IR active and five Raman active modes, in agreement with experimental data on a large number of spinels. Further, the influence of various types of crystallographic order upon the vibrational spectrum was considered; for example, if 1 : 3 ordering on octahedral sites takes place, the space group is reduced from O_4^7 to O^7 and the number of IR active modes increases from 4 to 21. The occurrence of a fine structure on the IR spectrum can be considered as an indication of the presence of crystallographic ordering, even in the case that superstructure reflections in the X-ray diffractogramm are not observable because of nearly equal scattering powers of the ordered atoms.

In the $Li_{0.5}(CrFe)_xGa_{2.5-2x}O_4$ system, the order–disorder transition $P4_332 \rightarrow Fd3m$ occurs for $1 < x < 1.25$, i.e., with the beginning of the migration of Li^+ cations from octahedral to tetrahedral sites. It is remarkable that the long range 1 : 3 order does not seem disturbed by introducing three trivalent cations; only the valency of the cation seems to be important, which points out that the main force of the ordering must be searched in the anion polarization energy caused by the differences in ionic charge of the cations.

Infrared spectra of spinels with 1 : 3 order on the octahedral sites are shown in Fig. 3. There are 15 bands for $Li_{0.5}Ga_{2.5}O_4$, including several apparent shoulders that could not be resolved. The agreement between the earlier measurements (31, 34) and those reported here is quite good except for small changes in relative intensity. The

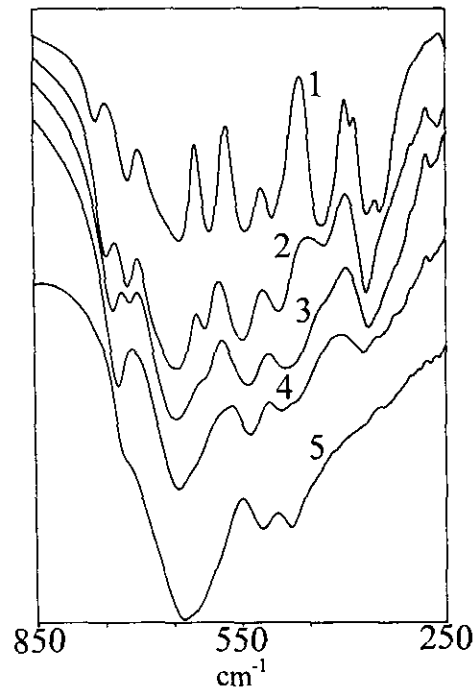

FIG. 3. Determination of the order–disorder transition $P4_332 \rightarrow Fd3m$ by infrared spectroscopy in the $Li_{0.5}(FeCr)_xGa_{2.5-2x}O_4$ system. 1, $x = 0$; 2, $x = 0.5$; 3, $x = 0.75$; 4, $x = 1$; and 5, $x = 1.25$.

TABLE 6
IR Frequencies (in cm^{-1}) of the $Li(CrFe)_xGa_{2.5-2x}O_4$ Solid Solutions

Composition	Frequencies											
$Li_{0.5}Ga_{2.5}O_4$	761	713	639	595	538	502(14)	490	424	415	389	360	348
$x = 0.25$	754	714	640	598	544	496(26)		425			363	
$x = 0.5$	745	714	642	602	548	494(21)		428			365	
$Li_{0.5}Cr_{0.5}Ga_2O_4$	755	720	643	607	555	502(24)		433			369	
Difference (with $Li_{0.5}Ga_{2.5}O_4$)	−6	+7	+4	+12	+17	—		+9			+9	
$Li_{0.5}Fe_{0.5}Ga_2O_4$	750	708	633	589	535	498		426			357	
Difference	−11	−5	−6	−6	−3	−4		+2			−3	

Note. (14) $\Delta\nu$: ^6Li–^7Li isotopic shift.

details of the spectra, particularly the degree of resolution of the bands, are sensitive to the method of preparation to some extent (the observed nonreproducibility is related to the granulometry of the sample).

The isomorphic replacement of the tetrahedral gallium by iron and that of the octahedral gallium by iron and chromium in $Li_{0.5}Ga_{2.5}O_4$ induces a progressive disappearance of bands located at 348, 389, 424, 595, and 714 cm^{-1} and a general shift (5–15 cm^{-1}) of the other frequencies related to the presence of octahedral chromium (Table 6). The greatest frequency differences are found for the bands located near 540 and 600 cm^{-1}; these frequencies are characteristic of the two high-frequency bands ν_1 and ν_2 of chromites (35).

	Frequency (in cm^{-1})	
	ν_1	ν_2
MCr_2O_4 (M = Mn, Co, Ni, Zn)	620–635	512–537

It is evident from the isotopic data that one band only is strongly shifted in the spectrum of the corresponding ^6Li–^7Li isotopic compounds and this may be assigned to a translation of the lithium cation. Nevertheless, the isotopic frequency ratio (~1.04–1.05) is lower than the calculated value 1.08 for an isolated LiO_6 octahedron and, consequently, the LiO_6 and $M^{III}O_6$ vibrations are more or less mixed up. In pure spinels ($Li_{0.5}M_{2.5}O_4$, M = Al, Ga, and Fe) (22), the LiO_6 vibrations cannot be identified with the help of ^6Li–^7Li isotopic replacement (36).

Analysis of the Fe^{3+}_{tetra}–O–Cr^{3+}_{octa} Interaction Influence on the Electronic Spectrum

The strong intensification of the absorption observed in the range 13,000–20,000 cm^{-1} on the optical spectrum for $x \geq 0.75$ may be unambiguously correlated with the magnetic transition (Fig. 4).

Figures 5a and 5b show the absorption spectrum of the $Li_{0.5}Cr_{0.25}Fe_{0.25}Ga_2O_4$ compound (curve 1) from which the spectrum of the corresponding chromi- or ferrigallate (curves 2) has been subtracted to yield the final difference spectra (curves 3). The evolution of the two difference spectra with increasing values of x appears on Fig. 6.

In compounds where the $3d^3$ and $3d^5$ ions are diluted all the bands expected are observed but, from $x = 0.5$ to 1.25, the progressive growth of a large band near 15,000 cm^{-1} makes the other bands indistinguishable. Nevertheless, the electronic spectra of the latest compounds may be interpreted by means of the difference spectra (Table 7). The assignments proposed hereafter for the spectra of compounds with small values of x are confirmed by the analysis of the difference spectra.

	Energy and assignment of observed bands (in 10^3 cm^{-1})						
Compound	Fe^{3+}	Cr^{3+}	Cr^{3+}	Cr^{3+}	Fe^{3+}	Cr^{3+}	Fe^{3+}
	$^6A_1 \rightarrow {}^4T_1$	o_a	o_b	o_1	$^6A_1 \rightarrow {}^4E, {}^4A_1$	o_2	$^6A_1 \rightarrow {}^4E(D)$
$Li_{0.5}Cr_{0.25}Fe_{0.25}Ga_2O_4$	9.4	14.35	15.0	16.6	21.1	24.1	25.6

The two difference spectra reveal the same unknown band at about 14,500 cm^{-1} strongly enhanced for $x > 0.5$, i.e., in ferrimagnetic compounds at room temperature. This band is attributed to an electronic transition assigned to the $Cr^{3+} + Fe^{3+} \rightarrow Cr^{4+} + Fe^{2+}$ intervalence charge transfer.

Apart from the ligand field transitions, the most common

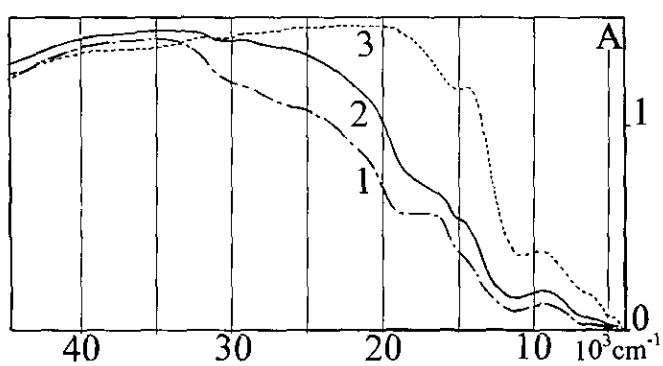

FIG. 4. Electronic spectra of $Li_{0.5}(CrFe)_xGa_{2.5-2x}O_4$ compounds. 1, $x = 0.25$; 2, $x = 0.5$; and 3, $x = 1$.

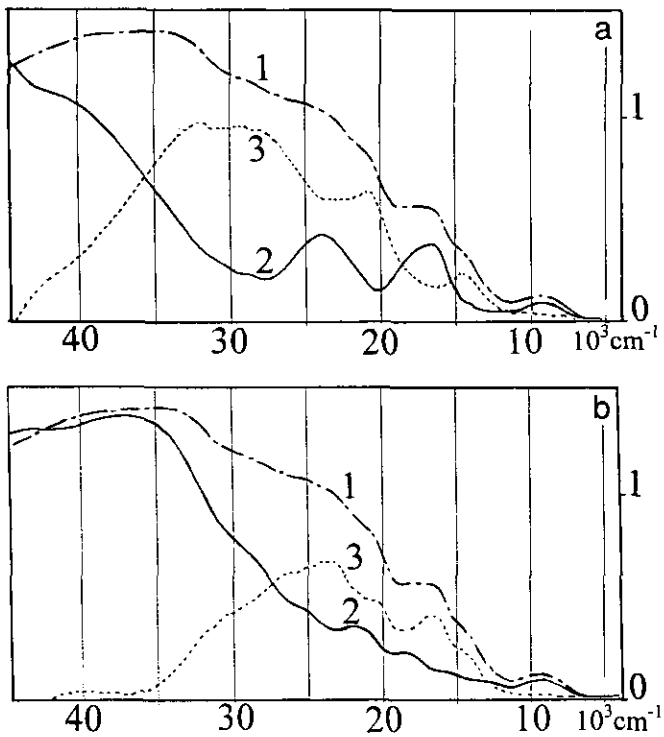

FIG. 5. (a) Electronic spectra of $Li_{0.5}(CrFe)_{0.25}Ga_2O_4$ (curve 1), $Li_{0.5}Cr_{0.25}Ga_{2.25}O_4$ (curve 2), and difference spectrum (curve 3). (Analysis of the difference spectra in Table 7.) (b) Electronic spectra of $Li_{0.5}(CrFe)_{0.25}Ga_2O_4$ (curve 1), $Li_{0.5}Fe_{0.25}Ga_{2.25}O_4$ (curve 2), and difference spectrum (curve 3). (Analysis of the difference spectra in Table 7.)

type of electronic transition observed in the visible to near infrared spectra of transition metal oxides and silicates is intervalence or metal–metal charge transfer. Such transitions involve the transfer of an electron from one metal cation to another. Among minerals, the most common example is $Fe^{2+} \rightarrow Fe^{3+}$ charge transfer in mixed valence iron oxides and silicates.

Intervalence charge transfer can also occur between different metal cations, the most common mineralogical example being the Fe–Ti charge transfer:

$$Fe^{2+} + Ti^{4+} \rightarrow Fe^{3+} + Ti^{3+}$$

Iron-titanium charge transfer results in an intense absorption band centered near 20,000 cm^{-1} in the spectra of Fe–Ti oxides and silicates.

In a series of papers, Sherman has investigated the nature of $Fe^{2+} \rightarrow Fe^{3+}$ (37), $Fe^{2+} \rightarrow Ti^{4+}$ (38), and $Mn^{3+} \rightarrow Fe^{3+}$ (39) charge transfers using spin-unrestricted self-consistent field-Xα-scattered wave molecular orbital calculations in $(Fe_2O_{10})^{15-}$, $(FeTiO_{10})^{14-}$, and $(FeMnO_{10})^{14-}$ clusters. The theoretical values of energy for these charge transfers are in reasonable agreement with the energies observed in the optical spectra of oxides and silicates (Table 8).

The phenomena observed in mixed oxides of corundum and spinel structures ($CrFeO_3$, $Li_{0.5}Fe_{0.5}Cr_2O_4$ (29), $Li_{0.5}(CrFe)_xGa_{2.5-2x}O_4$ $x \geq 0.75$, this paper) cannot be described in general terms but we can arrive at the following argument. The energy required for a charge transfer $Fe^{3+} + Cr^{3+} \rightarrow Fe^{2+} + Cr^{4+}$ will depend on the energy difference $IP(IV)_{Cr} - IP(III)_{Fe}$ where $IP(N)$ denotes the ionization potential required to reach the N-charged species from the $(N - 1)$ charged species. In a crystal this difference will be modified by a certain factor and other effects (e.g., crystal-field stabilization) have to be considered too.

	Ionization potential (eV)		
Element	2nd	3rd	4th
Cr	16.49	30.95	49.6
Mn	15.64	33.69	52
Fe	16.18	30.64	57.1

The difference of more than 7 eV between IP(IV) of chromium and iron indicates that the charge transfer studied in this paper corresponds unambiguously to the reaction $Fe^{3+} + Cr^{3+} \rightarrow Fe^{2+} + Cr^{4+}$. The experimental energies observed for optically induced $Fe^{3+} \rightarrow Cr^{3+}$ and $Mn^{3+} \rightarrow$

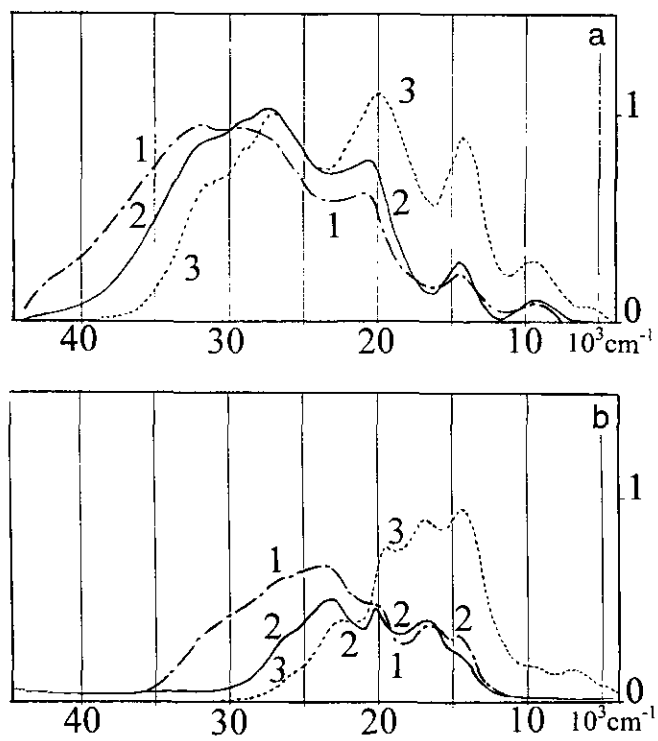

FIG. 6. Difference spectra near the magnetic transition. (a) Between $Li_{0.5}(CrFe)_xGa_{2.5-2x}O_4$ and $Li_{0.5}Cr_xGa_{2.5-x}O_4$. (b) Between $Li_{0.5}(CrFe)_xGa_{2.5-2x}O_4$ and $Li_{0.5}Fe_xGa_{2.5-x}O_4$. 1, $x = 0.25$; 2, $x = 0.5$; and 3, $x = 1$.

TABLE 7
Analysis of the Difference Spectra (Energy in (10^3 cm^{-1}) and Assignment of Observed Bands)

$Li_{0.5}(CrFe)_xGa_{2.5-2x}O_4$–$Li_{0.5}Cr_xGa_{2.5-x}O_4$

x	Fe^{3+} $^6A_1 \rightarrow {}^4T_1$	IVCT and Fe^{3+} $^6A_1 \rightarrow {}^4T_2$	$^6A_1 \rightarrow {}^4E_1$ $^4A_1$	Fe^{3+}	and	Cr^{3+} pair transitions	
0.25	9.6	14.6	20.8	28.4[b]		29.4	30.6
0.5	9.6	14.6	20.7	27.5[c]		29	30.5
1	9.5	14.3	20[a]	27.1[c]		29	30.6

$Li_{0.5}(CrFe)_xGa_{2.5-2xO4}$–$Li_{0.5}Fe_xGa_{2.5-x}O_4$

x		IVCT and Cr^{3+} o_a, o_b	Cr^{3+} o_1	Fe^{3+} transition[d]	Cr^{3+} o_2	Cr^{3+} ligand field parameters $10Dq$	B_{35}
0.25		~14.5	16.7	20.7	23.7	16.7	0.71
0.5		14.7	16.5	20	23.2	16.5	0.67
0.75		14.6	16.7	19.6	22.8	16.7	0.59
1	7.1	14.4	16.8	19.5	22.5	16.8	0.54_5

Note. 14.6, 23.7 main band.
[a] Composite of the ligand field $^6A_1 \rightarrow {}^4E_1$ $^4A_1$ and pair $2(^6A_1) \rightarrow 2(^4T_1)$ transitions.
[b] $2(^6A_1) \rightarrow (^4E_1$ $^4A_1) + {}^4T_1$ pair transition.
[c] Composite of the ligand field $^6A_1 \rightarrow {}^4E(D)$ and Fe^{3+} pair $2(^6A_1) \rightarrow 2(^4T_2)$ transitions.
[d] Assignment previously mentioned.

Fe^{3+} charge transfers are compatible with the theoretical calculations and seem to indicate that for other transition metal ions (except V^{3+}) this absorption band is at higher energies. The antiferromagnetic Fe^{3+}_{tetra}–O–Fe^{3+}_{octa} interactions induce in ferrimagnetic compounds the intensification of iron pair transitions: $^6A_1 \rightarrow {}^4E_1{}^4A_1$, $2(^6A_1) \rightarrow 2(^4T_1)(^4G)$ and $2(^6A_1) \rightarrow 2{}^4T_2(^4G)$ as in low Curie temperature compounds of $Li_{0.5}Fe_xGa_{2.5-x}O_4$ ($x = 1.25$ and 1.5). The Mössbauer spectra of $Li_{0.5}Fe_1Cr_1Ga_{0.5}O_4$ and $Li_{0.5}Fe_{1.5}Ga_1O_4$ are quite similar because octahedral Cr^{3+} is known to exhibit a small superexchange interaction in oxidic spinels.

The stronger antiferromagnetic interactions in $Li_{0.5}(CrFe)_xGa_{2.5-2x}O_4$ induce a more pronounced and rapid decrease of the Racah parameter B_{35} for Cr^{3+} octahedral than that observed in $Li_{0.5}Cr_xGa_{2.5-x}O_4$.

IV. CONCLUSION

Near infrared to near ultraviolet spectra in lithium ferrite spinels show bands due to ligand field and pair transitions whose energies are similar to those found in other iron oxides and oxide hydroxides. The tetrahedral and octahedral Fe^{3+} ligand field transitions are strongly intensified by magnetic coupling of adjacent Fe^{3+} in the crystal structure of these oxides. Both types of transitions are Laporte and spin-allowed via the magnetic coupling of adjacent Fe^{3+} cations. The A–B interactions between tetrahedral Fe^{3+} and octahedral Cr^{3+} in lithium ferrimagnetic spinels induce an intense electronic transition assigned to Cr^{3+} + Fe^{3+} → Cr^{4+} + Fe^{2+} intervalence charge transfer at 1.8 eV.

TABLE 8
Energy (in eV) of Theoretical and Experimental Data Relative to Metal–Metal Charge Transfer in Oxides and Silicates

$Fe^{2+} \rightarrow Fe^{3+}$			$Fe^{2+} \rightarrow Ti^{4+}$			$Mn^{3+} \rightarrow Fe^{3+}$		
Calc.	0.84 or 1.31			2.23			2.20	
Exp. 0.88	Fe_3O_4	(40)[a]	2.25	Ulvospinel	(41)	~1.75	$Li_{0.5}Fe_{2.5-x}Mn_xO_4$	(46)
1.18–1.61	MgO: Fe^{3+}	(41)	2.50	Ilmenite	(41)		($x \leq 0.25$)	
1.05	$Fe_{1.5}Al_{1.5}O_4$	(42)	2.58	Andalusite	(45)			
0.87–1.05	Mn(II) Ferrites	(43)	2.81–3.05	Tourmaline	(45)			
1.52	Ilvaite	(44)						
1.62	Rockbridgeite	(44)						

[a] Reference numbers in parentheses.

REFERENCES

1. J. A. Schulkes and G. Blasse, *J. Phys. Chem. Solids* **24,** 1651 (1963).
2. M. Lenglet, *Rev. Chim.* **2,** 217 (1965).
3. S. K. Kulshreshtha and G. Ritter, *J. Mater. Sci.* **20,** 3926 (1985).
4. K. P. Belov, A. N. Goryaga, and A. I. Kokorev, *Sov. Phys. Solid State* **25,** 1022 (1983).
5. Sh. Sh. Bashkirov, R. A. Iskhakov, A. B. Liberman, V. I. Sinyavskii, Yu. A. Memalui, and N. N. Efimova, *Sov. Phys. Solid State* **18,** 1498 (1976).
6. V. D. Doroshev, V. A. Klochan, N. M. Kovtum, and V. N. Seleznev, *Phys. Status Solidi* **26,** 77 (1974).
7. S. M. Zhilyakov, V. V. Ivolga, and E. P. Naiden, *Sov. Phys. Solid State* **20,** 1980 (1978).
8. G. T. Pott and B. D. McNicol, *J. Chem. Phys.* **56,** 5246 (1972).
9. N. T. Melamed, F. de S. Barros, P. J. Viccaro, and J. O. Artman, *Phys. Rev. B* **5,** 3377 (1972).
10. J. M. Neto, T. Abritta, F. de S. Barros, and N. T. Melamed, *J. Lumin.* **22,** 109 (1981).
11. T. Abritta and F. de S. Barros, *J. Lumin.* **40** and **41,** 187 (1988).
12. T. Abritta, F. H. Blak, and R. J. M. Da Fonseca, *Phys. Status Solidi B* **158,** K75 (1990).
13. X. X. Zhang, J. Schoenes, W. Reim, and P. Wachter, *J. Phys. C: Solid State Phys.* **16,** 6055 (1983).
14. J. Ferguson and P. E. Fielding, *Aust. J. Chem.* **25,** 1371 (1972).
15. D. M. Sherman and T. Waite, *Am. Mineral.* **70,** 1262 (1985).
16. M. Lenglet, M. Bizi, and C. K. Jørgensen, *J. Solid State Chem.* **86,** 82 (1990).
17. D. Sherman, *Phys. Chem. Miner.* **12,** 161 (1985).
18. E. Pollert, J. Hetjmanek, J. P. Doumerc, J. Claverie, and P. Hagenmuller, *J. Phys. Chem. Solids* **44,** 273 (1983).
19. L. G. J. de Hart, *J. Electrochem. Soc.* **132,** 2933 (1985).
20. G. Busca, G. Ramis, M. Prieto, and V. S. Escribano, *J. Mater. Chem.* **3,** 665 (1993).
21. J. Arsene, J. Lopitaux, M. Drifford, and M. Lenglet, *Phys. Status Solidi A* **52,** K111 (1979).
22. J. Arsene and M. Lenglet, *Mater. Res. Bull.* **15,** 1681 (1980).
23. H. Szymczak, M. Wardzynska, and I. E. Mylnikova, *J. Phys. C., Solid State Phys.* **8,** 3937 (1975).
24. M. P. Pietrov, H. Szymczak, R. Wadas, and W. Wardzynski, *J. Phys. (Paris) Coloq.* **C1**(32), C1–847 (1971).
25. M. Bizi, Thesis, Rouen, 1989.
26. J. Arsene, Thesis, Rouen, 1979.
27. D. Reinen, *Struct. Bonding* **6,** 30 (1969).
28. D. Reinen, *Z. Naturforsch A* **29,** 521 (1968).
29. M. Lenglet, F. Hochu, and S. Music, *Solid State Commun.* **24,** 211 (1995).
30. E. W. Gorter, *Philips Res. Rep.* **9,** 295, 321, and 403 (1954).
31. P. Tarte, *Mém. Acad. R. Belg.* **35,** 40a–b (1965).
32. W. B. White and B. A. Deangelis, *Spectrochim. Acta, A* **23,** 985 (1967); *J. Solid State Chem.* **3,** 358 (1971).
33. J. Preudhomme, *Ann. Chim.* **9,** 31 (1974); Thesis, Liège, 1971.
34. V. G. Keramidas, B. A. Deangelis, and W. B. White, *J. Solid State Chem.* **15,** 233 (1975).
35. J. Preudhomme and P. Tarte, *Spectrochim. Acta, A* **27,** 1817 (1971).
36. P. Tarte and R. Collongues, *Ann. Chim.* **9,** 135 (1964).
37. D. M. Sherman, *Phys. Chem. Miner.* **14,** 355 (1987).
38. D. M. Sherman, *Phys. Chem. Miner.* **14,** 364 (1987).
39. D. M. Sherman, *Am. Mineral.* **75,** 256 (1990).
40. R. G. J. Strens and B. J. Wood, *Mineral Mag.* **43,** 347 (1979).
41. G. Smith, *Phys. Status Solidi* **61,** K191 (1980).
42. M. Lenglet, J. Arsene, and F. Jeannot, *Rev. Chim. Miner.* **24,** 81 (1987).
43. F. Petit and M. Lenglet, *Solid State Commun.* **86,** 67 (1993).
44. G. Amthauer and G. R. Rossman, *Phys. Chem. Miner.* **11,** 37 (1984).
45. G. Smith, *Can. Mineral.* **15,** 500 (1977).
46. F. Hochu and M. Lenglet, unpublished results.